Proc. of the Intl. Conf. on Advances In Mechanical And Automation Engineering – MAE 2014.
Copyright © Institute of Research Engineers and Doctors. All rights reserved.
ISBN: 978-1-63248-022-4 doi: 10.15224/ 978-1-63248-022-4-52

The Roll Dynamics for High Speed Paper Manufacturing

R. Whalley

***Abstract*— The transverse, dynamic deflection of high speed, wide faced, composite tubular rolls is investigated. General procedures are proposed enabling the analysis of inter-connected units comprising both distributed parameter and rigid, point-wise models. Modelling methods, eliminating intermediate variables are employed facilitating the realization of an overall system, input – output representation. An illustrative study, detailing the analysis and evaluation process is presented. A high speed, MG paper making machine, table roll application is considered. Whirling conditions and the effect of this problem on sheet quality and manufacturing output is commented upon.**

***Keywords*— wide, tubular, rolls, whirling, speed**

I. Introduction

The wide faced rolls used in high speed, sequential, paper and board manufacturing operations are investigated. These elements are costly to produce and maintain owing to exacting specification requirements, surface finish quality and their dynamic characteristics, see for example, [1], [2].

Typically, machine speeds of up to 6,500 ft/min are encountered in these industries where continuous production schedules spanning two to three weeks are usually required. To accommodate the sheet specification tolerances imposed, roll cambering, so that upon sagging the roll, contact profile is free from deflection, is regularly achieved via contouring, during final roll turning, grinding and polishing operations.

Without these fine limits manufacturing consistency, sheet thickness, strength and absorbency etc. would be compromised. Of equal importance, interruptions in production owing to uneven wear, differential loading and sheet tearing may be experienced resulting in expensive shut-down, maintenance and refit costs.

Costs, mass-inertia and dynamic deflection penalties are also instrumental in minimizing the tube wall thicknesses, of the many machine rolls used in these industries, at the design stage. Unfortunately, this also invites elastic deformation and dynamic deflection and both of these effects are constantly excited owing to internally generated noise, shock and vibration, as detailed in [3], [4].

Professor Robert Whalley, Professor of Engineering
The British University in Dubai,
P.O. Box 345015, Dubai-UAE,

These variations are difficult to suppress in practice following initial design, installation and commissioning. However, the tendency towards wider machine construction elevated operating speeds and capital cost economies all promote and contribute to machine vibration, as in [5] and this remains as an endemic problem.

In this regard, the effect of transverse vibrations when employing wide faced rolls is difficult to counter. Ultimately addressing this problem during the design process, see for example [6], is of fundamental importance.

Otherwise, the manifestation of dynamic bowing, with the onset of whirling conditions, perpetrates breakdowns, production and consistency problems. This is an active operational condition which would not be detected via static inspections and from steady state measurements, as discussed in [7], [8].

II. Distributed-Lumped Parameter Roll Models

The roll models considered herein, and in practice have the structure shown in figure 1. Essentially, the central roll body comprises a thin walled tube. Both the left and right ends of the roll consist of cast iron centres with sold steel shafts which are supported by bearings, as considered in [9].

In the analysis following, the bearing shafts and tube elements will be treated as relatively rigid elements with lumped inertia and stiffness properties. The cast iron centres at each end of the assembly will also be assumed to be relatively rigid discs so that dynamically the arrangement comprises a lumped, lumped, distributed, lumped, lumped configuration, for analysis purposes as in [10].

The flexible, distributed parameter shafts and tubes may be described in terms of the deflection y, slope θ, bending moment m and shear force q at their left and right ends respectively. The derivation of the matrix equation for a parallel, flexible, distributed parameter tube element is presented in [11].

As a consequence for the left half tube, of length $l_1/2$, external diameter d_o, internal diameter d_i the governing equation, is:

$$\left(Y_4(s),\theta_4(s),M_{y4}(s),Q_{y4}(s)\right)^T=\mathbf{F}(s)\left(Y_3(s),\theta_3(s),M_{y3}(s),Q_{y3}(s)\right)^T \quad (1)$$

where in (1);

SEEK DIGITAL LIBRARY

Proc. of the Intl. Conf. on Advances In Mechanical And Automation Engineering – MAE 2014.
Copyright © Institute of Research Engineers and Doctors. All rights reserved.
ISBN: 978-1-63248-022-4 doi: 10.15224/ 978-1-63248-022-4-52

$$\mathbf{F}(s)=\begin{bmatrix} f_1 & \frac{1}{2\gamma}f_2 & -\frac{Cl^2}{2\gamma^2}f_3 & -\frac{Cl^3}{2\gamma^3}f_4 \\ -\frac{\gamma}{2l}f_4 & f_1 & -\frac{Cl}{2\gamma}f_2 & -\frac{Cl^2}{2\gamma^2}f_3 \\ \frac{\gamma^2}{2l^2C}f_3 & \frac{\gamma}{2l}f_4 & f_1 & \frac{1}{2\gamma}f_2 \\ \frac{\gamma^3}{2Cl^3}f_2 & \frac{\gamma^2}{2l^2C}f_3 & -\frac{\gamma}{2l}f_4 & f_1 \end{bmatrix}$$

and:

$$f_1=(\cosh\gamma+\cos\gamma)/2 \quad (2)$$

$$f_2=\sinh\gamma+\sin\gamma \quad (3)$$

$$f_3=\cosh\gamma-\cos\gamma \quad (4)$$

and

$$f_4=\sinh\gamma-\sin\gamma \quad (5)$$

where in equations (2) to (5):

$$\gamma=\Gamma^{1/2}l \quad (6)$$

l = length of the distributed parameter roll with:

$$\Gamma^{1/2}=s^{1/2}(LC)^{1/4}, \quad (7)$$

$$C=1/EI \quad (8)$$

and: $L=\rho A$ (9)

III. Fundamental Matrix Truncation

From (2) to (5) it is clear that the truncated forms for f_1, f_2, f_3 and f_4 are:

$$f_1=1+\frac{\gamma^4}{4!}+\frac{\gamma^8}{8!}+\ldots \quad (10)$$

$$f_2=2\left(\gamma+\frac{\gamma^5}{5!}+\frac{\gamma^9}{9!}+\ldots\right) \quad (11)$$

$$f_3=\gamma^2+2\frac{\gamma^6}{6!}+2\frac{\gamma^{10}}{10!}+\ldots \quad (12)$$

and

$$f_4=2\left(\frac{\gamma^3}{3!}+\frac{\gamma^7}{7!}+\frac{\gamma^{11}}{11!}+\ldots\right) \quad (13)$$

Substituting for f_1, f_2, f_3 and f_4 in (1) results in the elements of $\mathbf{F}(s)$ becoming:

$$f_{11}(s)=f_1=1+\frac{\gamma^4}{4!}+\frac{\gamma^8}{8!}+\ldots$$

$$f_{21}(s)=-\frac{\gamma}{2l}f_4=-\frac{1}{l}\left(\frac{\gamma^4}{3!}+\frac{\gamma^8}{7!}+\frac{\gamma^{12}}{11!}+\ldots\right)$$

$$f_{31}(s)=\frac{\gamma^2}{2l^2C}f_3=\frac{1}{2l^2C}\left(\gamma^4+\frac{2\gamma^8}{6!}+\frac{2\gamma^{12}}{10!}+\ldots\right)$$

$$f_{41}(s)=-\frac{\gamma^3}{2Cl^3}f_2=-\frac{1}{Cl^3}\left(\gamma^4+\frac{\gamma^8}{5!}+\frac{\gamma^{12}}{9!}+\ldots\right)$$

$$f_{12}(s)=\frac{l}{2\gamma}f_2=l\left(1+\frac{\gamma^4}{5!}+\frac{\gamma^8}{9!}+\ldots\right)$$

$$f_{22}(s)=f_1=1+\frac{\gamma^4}{4!}+\frac{\gamma^8}{8!}$$

$$f_{32}(s)=\frac{\gamma}{2C}f_4=\frac{1}{C}\left(\frac{\gamma^4}{3!}+\frac{\gamma^8}{7!}+\frac{\gamma^{12}}{11!}+\ldots\right)$$

$$f_{42}(s)=\frac{\gamma^2}{2Cl^2}f_3=\frac{1}{Cl^2}\left(\gamma^4+\frac{2\gamma^8}{6!}+\frac{2\gamma^{12}}{10!}+\ldots\right)$$

$$f_{13}(s)=-\frac{Cl^2}{2\gamma^2}f_3=-\frac{Cl^2}{2}\left(1+\frac{2\gamma^4}{6!}+\frac{2\gamma^8}{10!}+\ldots\right)$$

$$f_{23}(s)=-\frac{Cl}{2\gamma}f_2=-Cl\left(1+\frac{\gamma^4}{5!}+\frac{\gamma^8}{9!}+\ldots\right)$$

$$f_{33}(s)=f_1=1+\frac{\gamma^4}{4!}+\frac{\gamma^8}{8!}+\ldots$$

$$f_{43}(s)=\frac{\gamma}{2l}f_4=\frac{1}{l}\left(\frac{\gamma^4}{3!}+\frac{\gamma^8}{7!}+\frac{\gamma^{12}}{11!}+\ldots\right)$$

$$f_{14}(s)=-\frac{Cl^3}{2\gamma^3}f_4=-Cl^3\left(\frac{1}{3!}+\frac{\gamma^4}{7!}+\frac{\gamma^8}{11!}+\ldots\right)$$

$$f_{24}(s)=-\frac{Cl^2}{2\gamma^2}f_3=-\frac{Cl^2}{2}\left(1+\frac{2\gamma^4}{6!}+\frac{2\gamma^8}{10!}+\ldots\right)$$

$$f_{34}(s)=\frac{l}{2\gamma}f_2=l\left(1+\frac{\gamma^4}{5!}+\frac{\gamma^8}{9!}+\ldots\right)$$

$$f_{44}(s)=f_1=1+\frac{\gamma^4}{4!}+\frac{\gamma^8}{8!}+\ldots$$

since:

$$\gamma=\Gamma^{1/2}l=s^{1/2}(LC)^{1/4}l$$

It is clear that every element $f_{i,j}(s)\ 1\le i,j\le 4$ is a rational function in s following the substitution for γ. However, this properly is maintained for all truncations, irrespective of the number of terms included in the series expansions of f_1, f_2, f_3 and f_4.

IV. Cast Iron, Steel Bearing Shaft and Tube Gyroscopic Model

The input-output vectors from the distributed parameter tube model, given in section 2 become the input-output vectors for the lumped parameter models. In this regard the model for a rigid rotor, with polar moment of inertia J and mass m, as shown in figure 1, would arise from the transformed relationship.

$$Y_3(s)=Y_2(s),\theta_3(s)=\theta_2(s)$$

$$M_{y3}(s)=-J\Omega(s\theta_2(s))+M_{y2}(s)$$

$$Q_{y3}(s)=ms^2Y_2(s)+Q_{y2}(s),$$

All of the relatively point-wise, rigid rotor equations are similar in that the deflections and slopes at the input and output ends are approximately equal. Also, the bending

SEEK DIGITAL LIBRARY

Proc. of the Intl. Conf. on Advances In Mechanical And Automation Engineering – MAE 2014.
Copyright © Institute of Research Engineers and Doctors. All rights reserved.
ISBN: 978-1-63248-022-4 doi: 10.15224/ 978-1-63248-022-4-52

moments and shear stress at the output ends are equal to those at the input end, minus the gyroscopic couple and plus the acceleration force, respectively.

Hence:

$$\left(Y_3(s),\theta_3(s),M_{y3}(s),Q_{y3}(s)\right)^T=\mathbf{R}_1(s)\left(Y_2(s),\theta_2(s),M_{y2}(s),Q_{y2}(s)\right)^T \quad (14)$$

and

$$\left(Y_7(s),\theta_7(s),M_{y7}(s),Q_{y7}(s)\right)^T=\mathbf{R}_2(s)\left(Y_6(s),\theta_6(s),M_{y6}(s),Q_{y6}(s)\right)^T$$

where in (14), since the roll is symmetrical about the vertical centre line:

$$\mathbf{R}(s)=\mathbf{R_1}(s)=\mathbf{R_2}(s)=\begin{bmatrix}1 & 0 & 0 & 0\\ 0 & 1 & 0 & 0\\ 0 & -J_c\Omega s & 1 & 0\\ m_c s^2 & 0 & 0 & 1\end{bmatrix}$$

Also, the steel bearing shafts are governed by:

$$\left(Y_2(s),\theta_2(s),M_{y2}(s),Q_{y2}(s)\right)^T=\mathbf{B}_1(s)\left(Y_1(s),\theta_1(s),M_{y1}(s),Q_{y1}(s)\right)^T \quad (15)$$

and

$$\left(Y_8(s),\theta_8(s),M_{y8}(s),Q_{y8}(s)\right)^T=\mathbf{B}_2(s)\left(Y_7(s),\theta_7(s),M_{y7}(s),Q_{y7}(s)\right)^T$$

where again in (15), for symmetrical configurations:

$$\mathbf{B}(s)=\mathbf{B_1}(s)=\mathbf{B_2}(s)=\begin{bmatrix}1 & 0 & 0 & 0\\ 0 & 1 & 0 & 0\\ 0 & -J_s\Omega s & 1 & 0\\ m_s s^2 & 0 & 0 & 1\end{bmatrix}$$

Also, the gyroscopic couple experienced by the roll tube is given by the equation:

$$\left(Y_6(s),\theta_6(s),M_{y6}(s),Q_{y6}(s)\right)^T=\mathbf{G}(s)\left(Y_5(s),\theta_5(s),M_{y5}(s),Q_{y5}(s)\right)^T \quad (16)$$

where in equation (16):

$$\mathbf{G}(s)=\begin{bmatrix}1 & 0 & 0 & 0\\ 0 & 1 & 0 & 0\\ 0 & -J_T\Omega s & 1 & 0\\ 0 & 0 & 0 & 1\end{bmatrix}$$

This completes the lumped parameter element modelling.

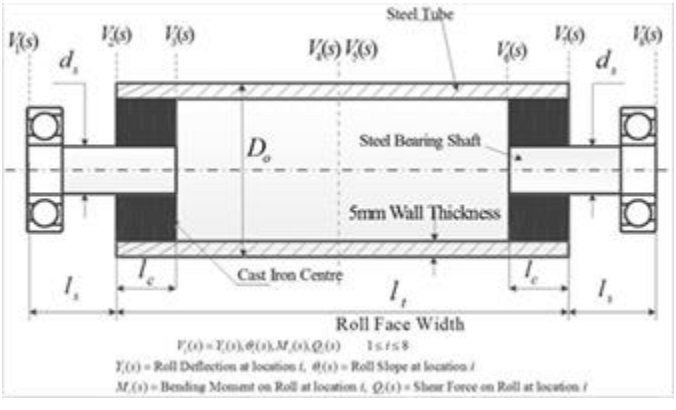

Figure 1, Roll General Arrangement

v. Overall Roll Model

A complete model for the overall roll can be easily assembled. If the equation for the left steel bearing shaft is:

$$\left(Y_2(s),\theta_2(s),M_{y2}(s),Q_{y2}(s)\right)^T=\mathbf{B}_1(s)\left(Y_1(s),\theta_1(s),M_{y1}(s),Q_{y1}(s)\right)^T \quad (17)$$

the equation for the left, cast iron centre is:

$$\left(Y_3(s),\theta_3(s),M_{y3}(s),Q_{y3}(s)\right)^T=\mathbf{R}_1(s)\left(Y_2(s),\theta_2(s),M_{y2}(s),Q_{y2}(s)\right)^T \quad (18)$$

followed by the left half tube equation:

$$\left(Y_4(s),\theta_4(s),M_{y4}(s),Q_{y4}(s)\right)^T=\mathbf{F}(s)\left(Y_3(s),\theta_3(s),M_{y3}(s),Q_{y3}(s)\right)^T \quad (19)$$

and gyroscopic equation:

$$\left(Y_5(s),\theta_5(s),M_{y5}(s),Q_{y5}(s)\right)^T=\mathbf{G}(s)\left(Y_4(s),\theta_4(s),M_{y4}(s),Q_{y4}(s)\right)^T \quad (20)$$

followed by the right half tube equation:

$$\left(Y_6(s),\theta_6(s),M_{y6}(s),Q_{y6}(s)\right)^T=\mathbf{F}(s)\left(Y_5(s),\theta_5(s),M_{y5}(s),Q_{y5}(s)\right)^T \quad (21)$$

with the right, cast iron centre equation of:

$$\left(Y_7(s),\theta_7(s),M_{y7}(s),Q_{y7}(s)\right)^T=\mathbf{R}_2(s)\left(Y_6(s),\theta_6(s),M_{y6}(s),Q_{y6}(s)\right)^T \quad (22)$$

and finally the right, steel bearing shaft equation is:

$$\left(Y_8(s),\theta_8(s),M_{y8}(s),Q_{y8}(s)\right)^T=\mathbf{B}_2(s)\left(Y_7(s),\theta_7(s),M_{y7}(s),Q_{y7}(s)\right)^T \quad (23)$$

completing the series component analysis.

vi. High Machine Table RollsConclusion

In this section the theoretical derivation given earlier will be applied to assess the whirling frequency of a high speed table roll. The parameters for this element, in accordance with Fig.1, are:

$2\text{m} \le l_t\,(\text{Roll face width}) \le 6\text{m}$

$0.08\text{m} \le D_o \le 0.2\text{m}$, roll tube wall thickness = 5mm

Tube material density: ρ_t = 7800 kg/m^3

Steel bearing shafts density: ρ_s = 7800 kg/m^3, l_s = 0.3 m, d_s = 0.02 m,

$J_s = 0.18378\times10^{-4}\,\text{kgm}^2$, m_s = 0.73514 kg.

For the steel tube: $C_t = 1/I_t E_t$ $L_t = \rho_t A_t$

In this case, from the dimensions given earlier, it is evident that the roll under consideration is symmetrical about the vertical centre line. Hence, as in Section 2:

$$\mathbf{B}_2(s)=\mathbf{B}_1(s)=\mathbf{B}(s) \text{ and } \mathbf{R}_2(s)=\mathbf{R}_1(s)=\mathbf{R}(s)$$

Upon eliminating intermediate variables, from equations (17) to (23):

$$\left(Y_8(s),\theta_8(s),M_{y8}(s),Q_{y8}(s)\right)^T=\mathbf{H}(s)\left(Y_1(s),\theta_1(s),M_{y1}(s),Q_{y1}(s)\right)^T, \quad (24)$$

$$\mathbf{H}(s)=\begin{bmatrix}\mathbf{I} & 0\\ \bar{\mathbf{B}}(s) & \mathbf{I}\end{bmatrix}\begin{bmatrix}\mathbf{I} & 0\\ \bar{\mathbf{R}}(s) & \mathbf{I}\end{bmatrix}\begin{bmatrix}\mathbf{F}_{11}(s) & \mathbf{F}_{12}(s)\\ \mathbf{F}_{21}(s) & \mathbf{F}_{22}(s)\end{bmatrix}\begin{bmatrix}\mathbf{I} & 0\\ \bar{\mathbf{G}}(s) & \mathbf{I}\end{bmatrix}\begin{bmatrix}\mathbf{F}_{11}(s) & \mathbf{F}_{12}(s)\\ \mathbf{F}_{21}(s) & \mathbf{F}_{22}(s)\end{bmatrix}\begin{bmatrix}\mathbf{I} & 0\\ \bar{\mathbf{R}}(s) & \mathbf{I}\end{bmatrix}\begin{bmatrix}\mathbf{I} & 0\\ \bar{\mathbf{B}}(s) & \mathbf{I}\end{bmatrix}$$

where:

SEEK DIGITAL LIBRARY

Proc. of the Intl. Conf. on Advances In Mechanical And Automation Engineering – MAE 2014.
Copyright © Institute of Research Engineers and Doctors. All rights reserved.
ISBN: 978-1-63248-022-4 doi: 10.15224/ 978-1-63248-022-4-52

$$\bar{\mathbf{B}}(s)=\begin{bmatrix}0 & -J_s\Omega s\\ m_s s^2 & 0\end{bmatrix},\ \bar{\mathbf{R}}(s)=\begin{bmatrix}0 & -J_c\Omega s\\ m_c s^2 & 0\end{bmatrix}$$

$$\text{and } \bar{\mathbf{G}}(s)=\begin{bmatrix}0 & -J_T\Omega s\\ 0 & 0\end{bmatrix}$$

where in equation (24) the partitions are in 2x2 block form and:

$$\mathbf{H}(s)=\begin{bmatrix}(\mathbf{F}_{11}+\mathbf{F}_{12})^2+\mathbf{F}_{12}\{\bar{\mathbf{G}}(\mathbf{F}_{11}+\mathbf{F}_{12}\mathbf{Z})+\mathbf{F}_{21}+\mathbf{F}_{22}\mathbf{Z}\} & (\mathbf{F}_{11}+\mathbf{F}_{12}\mathbf{Z})\mathbf{F}_{12}+\mathbf{F}_{12}(\bar{\mathbf{G}}\mathbf{F}_{12}+\mathbf{F}_{22})\\ (\mathbf{F}_{21}+\mathbf{F}_{22}\mathbf{Z})(\mathbf{F}_{11}+\mathbf{F}_{12}\mathbf{Z})+\mathbf{F}_{22}\{\bar{\mathbf{G}}(\mathbf{F}_{11}+\mathbf{F}_{12}\mathbf{Z})+\mathbf{F}_{21}+\mathbf{F}_{22}\mathbf{Z}\} & \mathbf{F}_{22}(\bar{\mathbf{G}}\mathbf{F}_{12}+\mathbf{F}_{22})\end{bmatrix}$$

where $\mathbf{Z}=\left[\bar{\mathbf{R}}(s)+\bar{\mathbf{B}}(s)\right]$

The boundary conditions, for the roll shown in figure 1, would require, for built-in ends, that:

$$\begin{bmatrix}Y_8(s)\\ \theta_8(s)\end{bmatrix}=\begin{bmatrix}Y_1(s)\\ \theta_1(s)\end{bmatrix}=\begin{bmatrix}0\\ 0\end{bmatrix}$$

Consequently:

$$\begin{bmatrix}0\\ 0\\ M_8\\ Q_8\end{bmatrix}=\begin{bmatrix}\mathbf{H}_{11}(s) & \mathbf{H}_{12}(s)\\ \mathbf{H}_{21}(s) & \mathbf{H}_{22}(s)\end{bmatrix}\begin{bmatrix}0\\ 0\\ M_1\\ Q_1\end{bmatrix} \tag{25}$$

A solution to (25) is only possible if:

$$\det\ \mathbf{H}_{12}(s)=0 \tag{26}$$

If only the leading term of f_1, f_2, f_3 and f_4 is employed then:

$$\mathbf{F}(s)=\begin{bmatrix}1 & 1 & \vdots & -C_t l_t^2/2 & -C_t l_t^3/6\\ \frac{-s^2}{6}L_t C_t l_t^3 & 1 & \vdots & -C_t l_t & -C_t l_t^2/2\\ \cdots & \cdots & \vdots & \cdots & \cdots\\ \frac{s^2}{2}L_t l_t^2 & \frac{s^2}{6}L_t l_t^3 & \vdots & 1 & 1\\ s^2 L_t l_t & \frac{s^2}{6}L_t l_t^2 & \vdots & \frac{-s^2}{6}L_t C_t l_t^3 & 1\end{bmatrix} \tag{27}$$

$$=\begin{bmatrix}\mathbf{F}_{11}(s) & \vdots & \mathbf{F}_{12}(s)\\ \cdots & \vdots & \cdots\\ \mathbf{F}_{21}(s) & \vdots & \mathbf{F}_{22}(s)\end{bmatrix}$$

and from equation (14) for the cast iron centres and steel bearing shafts:

$$\mathbf{Z}=\begin{bmatrix}0 & -(J_c+J_s)\Omega s\\ (m_c+m_s)s^2 & 0\end{bmatrix}$$

respectively. Upon substituting for $\mathbf{F}_{11}$, $\mathbf{F}_{12}$ etc:

$$\mathbf{H}_{12}(s)=(\mathbf{F}_{11}(s)+\mathbf{F}_{12}(s)\mathbf{Z})\mathbf{F}_{12}(s)+\mathbf{F}_{12}(s)(\bar{\mathbf{G}}(s)\mathbf{F}_{12}(s)+\mathbf{F}_{22}(s)) \tag{28}$$

and $\det \mathbf{H}_{12}(s)$ may be evaluated from the algebraic expression for $0\le s=i\omega\le\infty$. Alternatively, the complex matrix for:

$$\mathbf{H}_{12}(i\omega)=\mathbf{X}(\omega)+i\mathbf{Y}(\omega)$$

may be computed and $\det \mathbf{H}_{12}(i\omega)$ may be obtained for each frequency.

For the roll under consideration the Bode diagram for: $1/\det \mathbf{H}_{12}(i\omega)$ gives an indication of the resonant frequencies for constant diameter, variable roll face width**:**

In this case, for the roll shown in figure 1, with an outside diameter of 0.2m and roll wall thickness of 5mm, the dynamic magnification at resonance with Ω = 2500 RPM is shown in figure 2, for $2\text{m}\le l_t\le 6\text{m}$.

VII. Conclusion

The analysis techniques introduced herein, propose new methods which incorporate both the distributed and flexural properties of machine rolls together with the rotational velocity effects. As a result of this modular analysis procedure, rolls and rotor systems for any distributed-lumped modelling composition can be easily constructed.

Effectively, this allows the series assembly of rolls and rotors comprising elements of various diameters, tube wall thicknesses, lengths and materials. These may have significant elastic deformation and relatively rigid characteristics, reflecting thereby the actual properties of this form of roll-rotor arrangement.

The rolls which operate at the highest rotational velocity are located at the extreme ends of the operation, in paper manufacturing and conversion systems. In this regard, MG table and at the dry end of the process, winder rolls, are particularly vulnerable to dynamic deflection and bowing. The application study herein examines the critical speed problem for wide faced, MG Yankee machine, table rolls. Various face width and diameter units can be analyzed to provide comparisons.

As the graphical results show, the dynamic amplification encountered changes owing to the stabilizing gyroscopic couple which the rolls experience at higher velocities. However, the problem of accelerating to the operational speed, or running at a speed in the vicinity of resonance, would cause roll bowing which would not be detectable from static measurements for example. In order to avoid these problems by design, accurate methods of assessment and critical speed analysis need to be employed. Equally, as with the technique outlined herein, details of the dynamic amplification condition near to resonance needs to be determined, before construction.

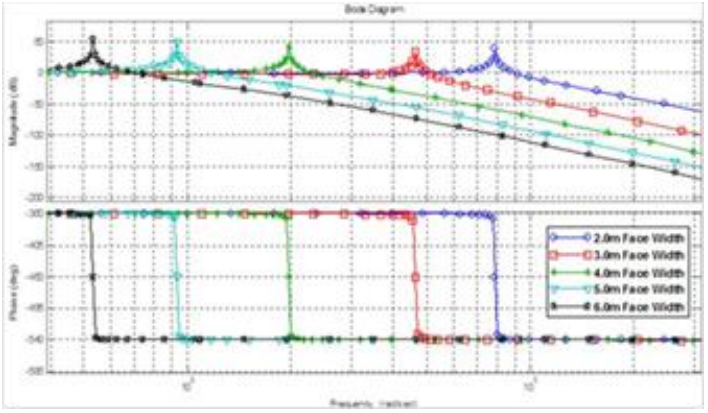

Figure 2, Bode diagram for $(1/\det \mathbf{H}_{12}(i\omega))$ with Ω=2500 RPM and $D_o=0.2\text{m}$, $D_i=0.19\text{m}$, $2\text{m}\le l_t$ (Roll Face Width) $\le 6\text{m}$

SEEK DIGITAL LIBRARY

Proc. of the Intl. Conf. on Advances In Mechanical And Automation Engineering – MAE 2014.
Copyright © Institute of Research Engineers and Doctors. All rights reserved.
ISBN: 978-1-63248-022-4 doi: 10.15224/ 978-1-63248-022-4-52

Acknowledgment

Professor Whalley wishes to acknowledge the support and encouragement for this research provided by the Vice Chancellor, The British University in Dubai-UAE.

References

[1] B. W. Smith, "Designing for Control of Papermaking Systems", Trans. British Paper and Board Maker Assoc., (ed. F Bowlam), Oxford, 1970.
[2] P.X. Long and J. S. Hsieh, Proc. Engineering and Paper Makers Conference, Nashville, 1997.
[3] C.E. Beards, "Engineering Vibration Analysis and Application", Edward Arnold, London, 1995.
[4] G. Genta, "Dynamics of Rotating Systems", Springer, New York, 2005.
[5] H. Bartlett and R. Whalley, "The Rotor Dynamics of Reeling Machinery", Applied Mathematical Modelling, Vol. 22, 1999, pp 1- 40.
[6] M. Aleyaasin, M. Ebrahimi and R. Whalley, "Vibration Analysis of Distributed – lumped Rotor Systems", Computer Methods in Applied Mechanics, 1999, pp 35-41.
[7] J.S. Rao, "Rotor Dynamics", J. Wiley, London, 2003.
[8] M. Aleyaasin, M. Ebrahimi and R. Whalley, "Multi-Mass Rotating Shaft Analysis and Identification", Proc. IMechE., pt K, Vol. 213, 1999, pp 73 – 85.
[9] R. Whalley and M. Ebrahimi, "Torsional Vibrations in Rotor Shells", Proc. IMechE., pt. C, Vol. 212, 1998, pp 263 – 276.
[10] H. Bartlett and R. Whalley, "Power Transmission System Modelling", Proc. IMechE. Pt. C, Vol. 212, No. 4, 1998, pp 497 – 508.
[11] R.J. Schwarz and R. Friedland, "Linear Systems", McGraw-Hill, New York, 1965.

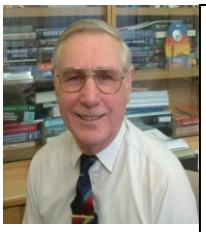

Robert Whalley is the Professor of Engineering at the British University in Dubai, since 2006. His research studies encompassed large-scale system modelling, simulation and control and distributed parameter analysis and design methods. This work has led to new multivariable, optimum, least effort, regulation strategies enabling the introduction of low gain, robust, feedback control and the accommodation of system parameter variations. Recent work advanced these techniques with the incorporation of adaptive control methods, for dispersed, systems with the toleration of non-linear, stochastic and spatial system, dynamic variations. During 1975-76 he was a visiting professor in marine system modelling and control in the Department of Engineering, at the University of Sao Paulo, Brazil**.** He was the Head of the Department of Mechanical and Medical Engineering from 1984-1999, University of Bradford, UK. In recognition of his research, he was awarded the degree of Doctor of Science (DSc) by the University of Manchester in

SEEK DIGITAL LIBRARY